

## A Nonlinear MIMO-PID Neural Controller Design for Vehicle Lateral Dynamics model based on Modified Elman Neural Network

M.Sc. Khulood E. Dagher

Al-Khwarizmi Collage of Engineering, University of Baghdad

Baghdad - Iraq

dagherkhulood@kecbu.uobagdad.edu.iq

### ABSTRACT

This paper presents a new design of a nonlinear multi-input multi-output PID neural controller of the active brake steering force and the active front steering angle for a 2-DOF vehicle model based on modified Elman recurrent neural. The goal of this work is to achieve the stability and to improve the vehicle dynamic's performance through achieving the desired yaw rate and reducing the lateral velocity of the vehicle in a minimum time period for preventing the vehicle from slipping out the road curvature by using two active control actions: the front steering angle and the brake steering force. Bacterial foraging optimization algorithm is used to adjust the parameters weights of the proposed controller. Simulation results based Matlab package show the control methodology has effectiveness performance in terms of the excellent dynamic behavior of the vehicle model by minimizing the tracking error and smoothness control signals without saturation state obtained, especially when adding a bounded external disturbances to the vehicle model.

**Keywords:** Modified Elman Neural Network; PID Controller; 2-DOF Vehicle Model; Bacterial Optimization Algorithm.

تصميم مسيطر عصبي تناسبي-تكامل- تفاضلي لا خطي متعدد الإدخال والإخراج لنموذج المركبة الجانبي الحركي مبني على أساس الشبكة العصبية ايلمن المعدلة

م. خلود اسكندر داغر

كلية هندسة الخوارزمي - جامعة بغداد

dagherkhulood@kecbu.uobagdad.edu.iq

### الخلاصة

إن هذا البحث يقدم تصميم جديد لمسيطر عصبي تناسبي تكاملي تفاضلي متعدد الإدخال والإخراج لقوة توجيه الفرامل الفعال ولتوجيه العجلات الأمامية الفعالة لنموذج المركبة (2-DOF) مبني على أساس الشبكة العصبية ايلمن المعدلة. إن الهدف الأساسي من هذا العمل هو تحقيق الاستقرارية وتحسين أداء الحركي للمركبة من خلال تحقق معدل الدوران المطلوب وتقليل السرعة الجانبية في اقصر وقت ممكن لمنع انزلاق المركبة خارج المنعطف باستخدام قوة توجيه الكبح وتوجيه العجلات الأمامية. لقد تم استخدام الخوارزمية الامثلية البكتيرية ليجاد وتعديل أوزان العناصر للمسيطر المقترح. من خلال نتائج المحاكاة باستخدام الحقيبة البرمجة ماتلاب تبين إن لهذا المسيطر أداء متين من حيث تصرف حركي ممتاز لنموذج المركبة بتقليل الخطأ التتابعي ونعومة إشارات السيطرة بدون الحصول على حالة الإشباع وبصورة خاصة عندما تم إضافة ضوضاء خارجية إلى نموذج المركبة.

**الكلمات الرئيسية:** الشبكة العصبية ايلمن المعدلة, المسيطر التناسبي التكاملي التفاضلي, نموذج المركبة (2-DOF), الخوارزمية الامثلية البكتيرية.



## 1. INTRODUCTION

Recently, intelligent vehicles give precious serve for both driver and passengers; they have played a very serious role in traveling safety, comfortably as well as they have reduced the risk of traffic problems. Since the vehicles confront unexpected parameter such as rain, side air force, vehicle wear, road condition, tire pressure loss and external disturbance, different automatic control systems have been developed in a modern car to prevent the spinning, drifting and rolling problems in order to help the driver to keep control on vehicle and to effectively reduce accident by using the modern automotive system technology such as Vehicle Dynamics Control (VDC), Anti-lock Brake System (ABS), Acceleration Slip Regulation (ASR) System, Electronic Stabilization Program (ESP) and Automatic Guidance Control (AGC), **Youngjin, et al., 2017 and Aalizadeh, et al., 2016.**

Thus, many researchers address different ways to control the steering and yaw rate some of these researches are: in, **Chen-Sheng, et al., 2012**, a robust control algorithm which consists of fuzzy neural network for automatic steering vehicle was introduced. In **Mumin, et al., 2014**, a robust PID controller for automated path following steering control driving was presented. In addition to that, **Hongliang, et al., 2010**, designed a sliding mode and back stepping yaw stability controller to make the vehicle yaw rate follow its reference based on model of vehicle yaw rate and wheel dynamics. Also in, **Haiping, et al. 2010**, a robust yaw moment controller for improving both handling and stability was proposed. In, **Ming, et al., 2012 and Bruin, et al., 2000**, the integral robust multi-tier model based back stepping vehicle steering control was explained. In, **Aalizadeh, et al., 2016**, a bee's algorithm and neural network were used as an efficient controller for front steering vehicle was proposed. In, **Gilles, et al., 2013**, a high order sliding mode control for autonomous vehicles was introduced. **Pan, et al., 2012**, designed an adaptive PID for autonomous vehicles control. **Hajjaji, et al., 2006 and Xianjian, et al., 2017**, showed a robust fuzzy controller for vehicle lateral dynamics. **Shijing, et al., 2008**, designed a genetic fuzzy neural network controller for four wheel steering. In **Guo, et al., 2014**, neural network slide mode controller for intelligent vehicle trajectory tracking was presented.

The motivation for this work is taken from **Haiping, et al., 2010, Youngjin, et al., 2017 and Aalizadeh, et al., 2016**: to investigate the stability of the vehicle dynamics by achieving the desired yaw rate and minimizing the lateral velocity to zero value in a short period of time for preventing the vehicle from sliding out the road curvature through designing a two active control actions: the front steering angle and the brake steering force.

The contribution of this research paper is a swift control action which is generated using MATLAB simulation based on the proposed design of the nonlinear MIMO-PID-MENN control law and Bacterial foraging optimization algorithm that leads to achieve the yaw rate of the vehicle with minimum lateral velocity. In addition to that, it is distinguished by performance robustness for bounded disturbance effects.

The remainder of this paper is organized as follows: Section 2 described the mathematical model of 2-DOF vehicle. Section 3 presented the proposed of nonlinear PID-MENN controller with Bacterial foraging tuning algorithm. Section 4, the performance of the numerical simulation results of the proposed control algorithm is illustrated. The conclusions are drawn in section 5.

## 2. MODEL OF VEHICLE LATERAL DYNAMICS

In general, the vehicle lateral dynamics motion is affected by many variables such as vehicle speed, vehicle mass and tires state on road, **Mark, et al., 2014**. In order to describe the mathematical vehicle later dynamics model and to achieve the stability of the system, the independent control of lateral and yaw motion requires at least one additional control input, the first one is the front steering angle and the second control signal is as one from three possible solutions as follows: rear wheel steering angle; braking forces; and torque driving wheel, **Martin, et al., 2017**.

This paper focuses on the vehicle yaw rate and lateral velocity as the desired outputs and there are two control actions the front steering angle and the differential braking as inputs to the vehicle model.

**Fig. 1** shows the two DOF vehicle model and it is widely used for lateral control design and has been shown to provide accurate response characteristics compared to more complex models for conditions up to 0.3g lateral acceleration, **Haiping, et al., 2010** and **Hajjaji, et al., 2006**.

To describe the mathematical model of vehicle lateral motion with interaction dynamic behavior in multi-input multi-output system can be taken, **Mark, et al., 2014** and **Martin, et al., 2017**, as follows:

$$\begin{bmatrix} \dot{L}_v \\ \dot{Y}_r \end{bmatrix} = \begin{bmatrix} -\frac{C_f + C_r}{MU} & -\frac{C_f a - C_r b}{MU} - MU \\ -\frac{C_f a - C_r b}{IU} & -\frac{C_f a^2 + C_r b^2}{IU} \end{bmatrix} \begin{bmatrix} L_v \\ Y_r \end{bmatrix} + \begin{bmatrix} \frac{C_f}{M} & 0 \\ \frac{a C_f}{I} & \frac{T}{2I} \end{bmatrix} \begin{bmatrix} \delta_f \\ F_{BS} \end{bmatrix} \quad (1)$$

$$\begin{bmatrix} y_1 \\ y_2 \end{bmatrix} = \begin{bmatrix} 1 & 0 \\ 0 & 1 \end{bmatrix} \begin{bmatrix} L_v \\ Y_r \end{bmatrix} + \begin{bmatrix} d_{\delta_f} \\ 0 \end{bmatrix} \quad (2)$$

Where:

$L_v$  and  $y_1$ : represent the lateral velocity;  $Y_r$  and  $y_2$ : represent yaw rate;  $a$ : is (1 m) the distance from the center of mass to front axle.  $b$ : is (1.5 m) the distance from the center of mass to rear axle;  $T$ : is (1.5 m) the vehicle track;  $C_f$ : is (55000 N/rad) the front tire cornering stiffness;  $C_r$ : is (45000 N/rad) the rear tire cornering stiffness;  $g$ : is (9.81 m/sec<sup>2</sup>) the acceleration of gravity;  $I$ : is (1500 kg m<sup>2</sup>) the vehicle moment of inertia;  $M$ : is (1000 kg) the vehicle mass;  $\delta_f$ : is the front steering angle;  $F_{BS}$ : is brake steer force;  $d_{\delta_f}$ : is the dynamics disturbances.

The brake steer force  $F_{BS}$  in equation (1) can be described as in equations (3 and 4) as follows **Martin, et al., 2017**:

$$M_{BS} = \frac{T}{2} (F_{XR} - F_{XL}) \quad (3)$$

$$F_{BS} = F_{XR} - F_{XL} \quad (4)$$

where:

$M_{BS}$ : is brake steer moment.  $F_{XR}$  and  $F_{XL}$ : are front and rear longitudinal tire forces respectively.

### 3. NONLINEAR MIMO-PID-MENN CONTROL DESIGN

In general, the traditional PID controller cannot be used as efficient organizers to achieve the desired outputs for multi-input multi-output system with dynamic behavior interaction. In fact, the proposed controller must work properly and instantly for different roads curvature to prevent the vehicle from sliding out the road in real time. Therefore, the general nonlinear MIMO-PID-MENN controller structure will be designed as shown in **Fig. 2**, where the outputs of the nonlinear MIMO-PID-MENN controller automatically control the vehicle lateral motion by using the brake steering force and the front wheel steering angle during the vehicle rotation on the curvatures.

It consists of three parts:

The first part is the simple structure of the PID controller that has many abilities such as an applicability, high robustness performance and widespread use with three control gains parameters that can be optimized and adjusted during the on-line control process. The PID control equation is given by Eq. (6), **Al-Araji, 2014**.

$$u(t) = k_p e(t) + k_i \int_0^t e(t) d(t) + k_d \frac{de(t)}{dt} \quad (6)$$

where: the proportional gain ( $k_p$ ); the integral gain ( $k_i$ ); the derivative gain ( $k_d$ ); the control action ( $u(t)$ ) and the error signal ( $e(t)$ ).

The second part is modified Elman recurrent neural network which constructed from four layers and each has its own operation as explained below, **Al-Araji, et al., 2011**:

- Input Layer: It works as a buffer i.e. passes the data with scaling modification.
- Hidden layer: It contains the non-linear activation functions.
- Context layer: It works as a memory for the previous layer i.e. non-linear activation functions.
- Output layer: It represents a linear collector unit which adds the all fed signals with scaling modification.

The structure of nonlinear MIMO-PID-MENN controller is shown in **Fig.3**. The parameters weights of the proposed controller are:  $kp_{1,2}$ ,  $ki_{1,2}$  and  $kd_{1,2}$  hidden layers weights while the parameters weights in the context layers are  $Vc_{1,2}$ ;  $Li$ : Linear node activation function;  $H$ : Sigmoid nonlinear activation function.  $h_{c_{1,2}}^o(k)$ : are context unit outputs;  $h_{1,2}(k)$ : are hidden unit outputs;  $\alpha$ : is the self-connections feedback gain it is represented randomly between (0 to 1);  $\beta$ : is the connection weight from the hidden layer to the context layer it is represented randomly between (0 and 1);  $e_{Yr}(k)$  and  $e_{Lv}(k)$ : are input error signals;  $F_{BS}(k)$ : is the differential braking system control action signal;  $\delta_f(k)$ : is the front wheel steering angle control action signal. The proposed control law equation for both the brake steering force control signal and the front wheel steering angle control signal of the MIMO-PID-MENN controller for the vehicle lateral dynamics motion are as follows:

$$\delta_f(k) = h_1(-) - h_2(-) \tag{7}$$

$$F_{BS}(k) = h_2(-) - h_1(-) \tag{8}$$

The outputs  $h_{1,2}(-)$  of the modified Elman neural network as in equations (9 and 10) depend on the sigmoid activation function, **Al-Araji, 2015**:

$$h_1(-) = \frac{2}{1 + e^{-net_1(-)}} - 1 \tag{9}$$

$$h_2(-) = \frac{2}{1 + e^{-net_2(-)}} - 1 \tag{10}$$

$net_{1,2}(-)$  are calculated from these equations (11 and 12), respectively:

$$net_1(-) = (kp_1 \times (e_{Yr}(k) + ki_1 \times (e_{Yr}(k) - e_{Yr}(k-1)) + kd_1 \times (e_{Yr}(k) - e_{Yr}(k-1))) + (Vc_1 \times h_{c_1}^o(k)) \tag{11}$$

$$net_2(-) = (kp_2 \times (e_{Lv}(k) + ki_2 \times (e_{Lv}(k) - e_{Lv}(k-1)) + kd_2 \times (e_{Lv}(k) - e_{Lv}(k-1))) + (Vc_2 \times h_{c_2}^o(k)) \tag{12}$$

Where:

$$h_{c_1}^o(k) = \alpha h_{c_1}^o(k-1) + \beta \delta_f(k-1) \tag{13}$$

$$h_{c_2}^o(k) = \alpha h_{c_2}^o(k-1) + \beta F_{BS}(k-1) \tag{14}$$

So, the feedback nonlinear MIMO-PID-MENN controller is very necessary to track and stabilize the tracking error in each of the lateral velocity and the yaw rate for the vehicle model outputs by using two control signals front steering angle and braking force.

Therefore, the new proposed nonlinear MIMO-PID-MENN has considerable properties which can be summarized by :

- Fast learning, high adaptation performance, high order control performance and this is due to the context units in MENN which memorize the previous activations of the hidden units.
- Good dynamic characteristic, no output oscillation and strong robustness performance and it is due to the self-connections in the context units which increase the order of the controller model.

In this work, a scaling factor  $S_F$  is needed to be added in the output layer for the MIMO-PID-MENN controller to convert the scaled values to actual values and it is equal to 5000 because the maximum value of the differential braking system control action for this model is equal to 5000 N. The parameters weights of the MIMO-PID-MENN controller  $kp_{1,2}$ ,  $ki_{1,2}$ ,  $kd_{1,2}$ , and  $Vc_{1,2}$  will be on-line adjusted by using Bacterial foraging optimization algorithm.

The third part is Bacterial foraging optimization algorithm which is proposed by **Passino, 2002**, it was considered a successful foraging strategy because of the notion of the natural selection which tended to eliminate the animals as well as it can be defined as a swarm intelligence technique because it had an individual and group foraging policies of the (E. Coli) bacteria in human intestine, **Das, et al., 2009**, as shown in **Fig. 4**.

The E. Coli bacteria is one of bacterial types, so it is always trying to find the best place by using two kinds of motion (swim or tumble) in order to get a high nutrient level and to avoid noxious places as shown in **Fig. 5, Das, et al., 2009**. The first motion is forward swimming or running when E. Coli bacteria are moving at a very fast rate in the direction of higher nutrient level and it is called “chemo-taxis”. The second motion is tumbling in uncertain direction with a very small displacement movement when the bacteria are arrived in a place with a lower nutrient level, **Munoz, et al., 2010**.

In general, Bacterial foraging optimization theory is explained by moving in the direction of nutrient value, where every bacterium releases chemical substances of attractant when heading to a nutritious place and repellent when they are near a noxious place and the following steps: Chemo-taxis, Swarming, Reproduction and Elimination and dispersal, **Das, et al., 2009 and Munoz, et al., 2010**.

**Chemo-taxis Step:** the equation that described the E. coli cell movement through swimming or tumbling via flagella as in Eq. (15):

$$P(i, (j + 1), k, l) = P(i, j, k, l) + C(i)\phi(i) \quad (15)$$

Where:

$P(i, j, k, l)$  : is the  $i^{th}$  bacterium position [ $kp_1$ ,  $ki_1$ ,  $kd_1$ ,  $kp_2$ ,  $ki_2$ ,  $kd_2$ ,  $Vc_1$  and  $Vc_2$ ] at the  $j^{th}$  chemo-taxis at  $k^{th}$  reproduction and  $l^{th}$  elimination and dispersal step.

$C(i)$  : is the step size of the tumble direction.

$\phi(i)$  : is the random of the length direction.

**Swarming Step:** this step gives the bacteria meet into groups to search the perfect path of food and reach the desired place quickly where every bacterium must be tried to attract other bacteria to make a high bacterial density by using Eq. (16):

$$J_{cc}(P(j, k, l), N(j, k, l)) = \sum_{i=1}^S J_{cc}^i(P(-), N(-)) \quad (16)$$

Where:

$J_{cc}(P(-), N(-))$  : is the cost function value.

$S$  : is the total number of bacteria.

$p$  : is the number of parameters to be optimized as  $P = [P_1, P_2, \dots, \theta_p]^T$ .

**Reproduction Step:** The healthier bacteria will generate two bacteria in the same location while the lower healthy bacteria ultimately die therefore, the swarm size is kept a constant.

**Elimination and Dispersal step:** in this step, the process of elimination and dispersal is very important to guarantee the diversity of new individuals and to find a place that may be near from a good food sources and in this algorithm the probability value to make the bacteria eliminated and dispersed is (0 to 1) where the elimination and dispersal probability value is denoted as ( $P_{ed}$ ).

The flowchart of the nonlinear MIMO-PID-MENN tuning control algorithm is shown in **Fig. 6**.

#### 4. SIMULATION RESULTS

The proposed MIMO-PID-MENN controller with tuning control algorithm based on Bacterial foraging optimization is carried out by Laptop computer simulation using Matlab package (2012) as m file program codes. In this paper, seven regions of operation have been taken depending on the variable speed of the vehicle as “15, 25, 35, 40, 30, 20 and 10” m/sec therefore, we have seven transfer functions for the dynamic model of the vehicle that was described in section two. So The desired lateral velocity for the dynamic model of the vehicle should be zero value in order to overcome the vehicle which may rotate around itself at high vehicle velocity while the desired yaw rate should be defined as in Eq. (17):

$$Y_{r_{des}}(k) = \frac{U(k)}{R} \quad (17)$$

Where:  $R$  is curvature radius and it is equal to 100 m.

It is very important to add scaling function at output of the proposed controller in order to overcome a numerical problem that is involved within real values by converting the scaled values to actual values where the differential braking range is  $\pm 5000$  N while the front steering angle is  $\pm 0.1$  rad.

To apply the proposed control scheme to the 2-DOF vehicle model, the proposed tuning control algorithm of BFO defined the parameters as follows:  $S$  is the total bacteria number and it equals to twenty;  $I$  the iteration number and it is equal to twenty;  $N_c$  is the number of chemo-tactic steps and it equals to ten;  $N_s$  is the swimming length and it equals to five;  $N_{re}$  is the number of reproduction steps and it equals to four;  $N_{ed}$  is the number of elimination-dispersal events and it equals to three;  $p_{ed}$  is the number of elimination-dispersal probability and it equals to 0.25 as proposed value and  $p$  is the cell number in BFO tuning algorithm and it equals to eight because of only eight parameters weights of MIMO-PID MENN controller to be adjusted.

To show the performance of the proposed MIMO-PID-MENN controller, there are seven steps change in the desired of yaw rate with sampling time is equal to 0.01 sec for minimum time constant from these seven transfer functions based on Shannon theorem while the desired lateral velocity is equal to zero.

**Fig. 7-a** observes the actual yaw rate output of the vehicle mode is fast tracking the desired yaw rate without overshoot state while the **Fig. 7-b** shows the actual lateral velocity of the vehicle that started from  $-2 \times 10^{-7}$  m/sec at very short transit state to zero value at steady state. The yaw rate error and lateral velocity error can be shown in **Figs. 8-a**, and **b**, respectively. **Figs. 9-a**, and **b** show the response of the two feedback control actions brake steer force “differential braking” and front steering angle respectively in order to achieve the desired yaw rate and to make the lateral velocity is equal to zero. The parameters weights of the nonlinear MIMO-PID-MENN controller have been adjusted and tuned in each state of the seven steps change in the desired yaw rate for the vehicle model, as shown in **Table 1**.

To confirm that the nonlinear MIMO-PID-MENN has a capability of the adaptation and robustness performance, a disturbance term  $\delta_{dis} = 2 \times 10^{-3} \sin(100t)$ , **Haiping, et al., 2010** has been added to the vehicle model that represents the dynamics disturbances. **Fig. 10-a** shows the response of the yaw rate of the vehicle which did not drift from the desired as well as it has very small overshoot while **Fig. 10-b** shows the lateral velocity of the vehicle that the response has a very small oscillation magnitude equals to  $\pm 0.008$  m/sec. The yaw rate error signal and lateral velocity error can be shown in the **Figs. 11- a**, and **b**, respectively for disturbance effects. The differential braking control signal and the front steering angle control signal of the nonlinear MIMO-PID-MENN for vehicle model with disturbance effect can be shown in **Figs. 12-a**, and **b**, respectively .



## 5. CONCLUSIONS

The nonlinear MIMO-PID-MENN controller with Bacterial foraging optimization algorithm for MIMO dynamic vehicle motion model has been presented in this paper. The yaw rate and lateral velocity are the state outputs of the 2-DOF vehicle model and they are excellent tracked the desired inputs because the proposed controller with BFO algorithm generated two control actions front steer angle and differential brake through finding and tuning the best and high stable parameters weights of the controller with minimum time and no oscillation in the output. Simulation results of lateral motion show that the effectiveness of proposed nonlinear MIMO-PID-MENN controller; this is demonstrated by the minimized tracking error of the lateral velocity and yaw rate to reach zero value in a short time period as well as the smooth control signal which has been obtained at different velocities of the vehicle model, especially when adding the external front steering angle disturbances problem.



## 6. REFERENCES

- Aalizadeh, B. and Asnafi, A., 2016, “*Integrated Bees Algorithm and Artificial Neural Network to Propose an Efficient Controller for Active Front Steering Control of Vehicles*”. International Journal of Automotive and Mechanical Engineering (IJAME). Vol. 13, No. 2, pp. 3476 - 3491.
- Al-Araji, A. , 2014, ”*Applying Cognitive Methodology in Designing On-Line Auto-Tuning Robust PID Controller for the Real Heating System*. Journal of Engineering. Vol. 20, No. 9, pp. 43-61.
- Al-Araji, A., 2015, “*A Cognitive PID Neural Controller Design for Mobile Robot Based on Slice Genetic Algorithm*”. Engineering & Technology Journal. Vol. 33, No. 1, pp. 208-222.
- Al-Araji, A., Abbod, M., Raweshidy, H., 2011, “*Design of a Neural Predictive Controller for Nonholonomic Mobile Robot Based on Posture Identifier*”. Proceedings of the IASTED International Conference Intelligent Systems and Control (ISC 2011), Cambridge, United Kingdom, pp.198-207.
- Bruin, D., Damen, A., Pogromsky, A. and Boschi, J., 2000, “*Backstepping Control for Lateral Guidance of All-wheel Steered Multiple Articulated Vehicles*”. IEEE Intelligent Transportation Systems Conference Proceedings Dearborn (MI), USA, pp. 95-100.
- Chen-Sheng, T., Yong-Nong, C., 2012, “*A Robust Fuzzy Neural Control Approach for Vehicle Lateral*”. Dynamics. Procedia Engineering, Vol. 29, pp. 479 – 483.
- Das, S., Biswas, A., Dasgupta, S. and Abraham, A., 2009 “*Bacterial Foraging Optimization Algorithm: Theoretical Foundations, Analysis, and Applications*”. Foundations of Computational Intelligence, Vol. 203 of the series Studies in Computational Intelligence, pp. 23-55.
- Gilles, T., Reine, T. and Ali, C. ,2013, “*Higher-Order Sliding Mode Control for Lateral Dynamics of Autonomous Vehicles with Experimental Validation*”. IEEE Intelligent Vehicles Symposium, Gold Coast, Australia, pp.678-683.
- Guo, L., Ping-shu, G., Yang, X. and LI, B., 2014, ”*Intelligent Vehicle Trajectory Tracking Based on Neural Networks Sliding Mode Control*”. International Conference on Informative and Cybernetics for Computational Social Systems (ICCSS), pp. 57-62.
- Haiping, D., Nong, Z. and Guangming, D.,2010, ”*Stabilizing Vehicle Lateral Dynamics With Considerations of Parameter Uncertainties and Control Saturation Through Robust Yaw Control*”. IEEE Transactions on Vehicular Technology, Vol. 59, No. 5, pp. 2593-2597.
- Hajjaji, A., Chadli, M., Oudghiri, M. and Pagès, O., 2006, ”*Observer-based Robust Fuzzy Control for Vehicle Lateral Dynamics*”. Proceedings of the 2006 American Control Conference Minneapolis, Minnesota, USA, pp. 4664-4669.
- Hongliang, Z. and Zhiyuan, L., 2010, “*Vehicle Yaw Stability-Control System Design Based on Sliding Mode and Backstepping Control Approach*”. IEEE Transactions on Vehicular Technology, Vol. 59, No. 7, pp. 3674-3678.
- Mark, W., Matthias, D. and Tobias. O, 2014, ”*State Estimation of Vehicle’s Lateral Dynamics using Unscented Kalman Filter*”. The 53<sup>rd</sup> IEEE Conference on Decision and Control. Los Angeles, California, USA, pp. 5015-5020.
- Martin, M. and Martin H., 2017, ”*Linear Analysis of Lateral Vehicle Dynamics*”. The 21<sup>st</sup> International Conference on Process Control (PC), Strbske Pleso, Slovakia. , pp. 240-246.
- Ming, X. and Mark, M., 2012, “*Backstepping Vehicle Steering Controller Using Integral and Robust Control Based on Dynamic State Estimation*”. IEEE/RSJ International Conference on Intelligent Robots and Systems, pp. 3132-3137.



- Mumin, E., Esmail, C., Bilin, G. and Levent, G., 2014,” *Robust PID Steering Control in Parameter Space for Highly Automated Driving*”. Hindawi Publishing Corporation International Journal of Vehicular Technology, Vol. 2014, pp. 1-8.
- Munoz, M., Halgamuge, S., Alfonso, W. and Caicedo, E., 2010, “*Simplifying the Bacteria Foraging Optimization Algorithm*”. The IEEE World Congress on Computational Intelligence, Barcelona, Spain, pp. 4095-4101.
- Pan, Z., Jiajia, C., Yan, S., Xiang, T., Tiejuan X. and Tao, M., 2012,” *Design of a Control System for an Autonomous Vehicle Based on Adaptive-PID*”. International Journal of Advanced Robotic Systems. Vol. 9, No. 44, pp. 1-11.
- Passino, K., 2002, “*Biomimicry of Bacterial Foraging for Distributed Optimization and Control*”. The IEEE Control Systems and Managements. pp. 52–67.
- Shijing, W., Enyong, Z., Ming, Q., Hui, R. and Zhipeng, L., 2008, “*Control of Four-Wheel-Steering Vehicle Using GA Fuzzy Neural Network*”. International Conference on Intelligent Computation Technology and Automation, pp. 869-873.
- Xianjian, J., Guodong, Y. and Junmin, W.,2017,” *Robust Fuzzy Control for Vehicle Lateral Dynamic Stability via Takagi-Sugeno Fuzzy Approach*”. American Control Conference Sheraton Seattle Hotel, Seattle, USA, pp. 5574-5579.
- Youngjin, J., Minyoung, L., In-Soo, S. and Kwanghee, N., 2017,”*Lateral Handling Improvement with Dynamic Curvature Control for an Independent Rear wheel Drive EV*”. International Journal of Automotive Technology, Vol. 18, No. 3, pp. 505–510.

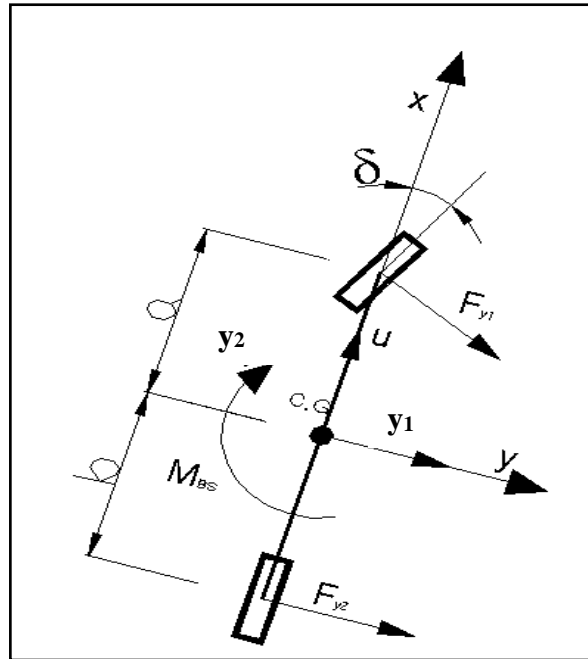


Figure 1. The Schematic diagram of two DOF Vehicle Models.

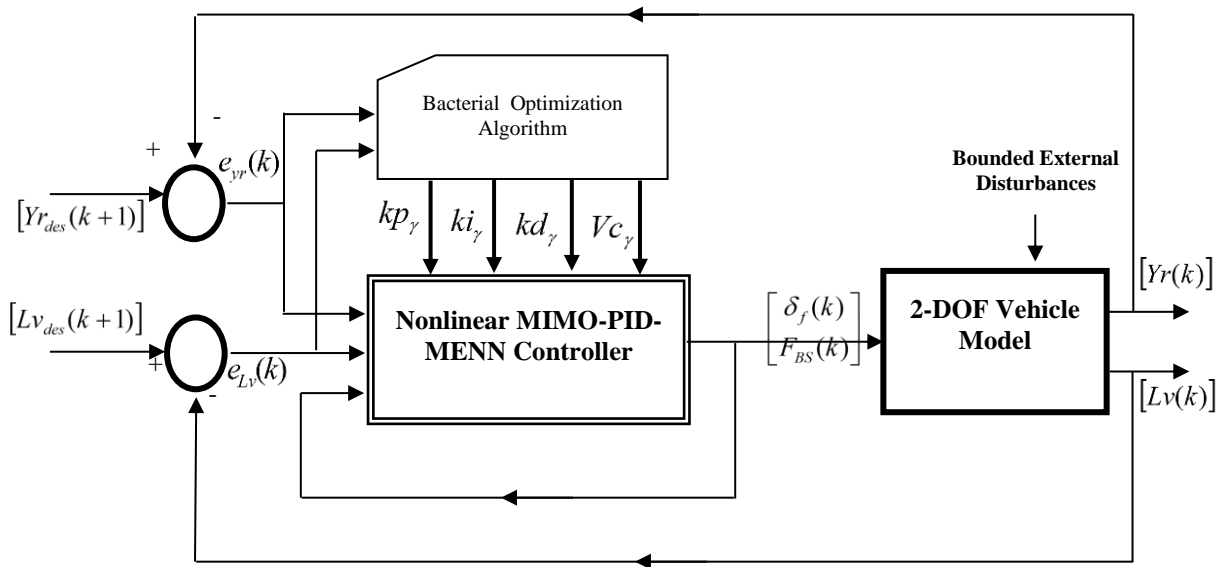
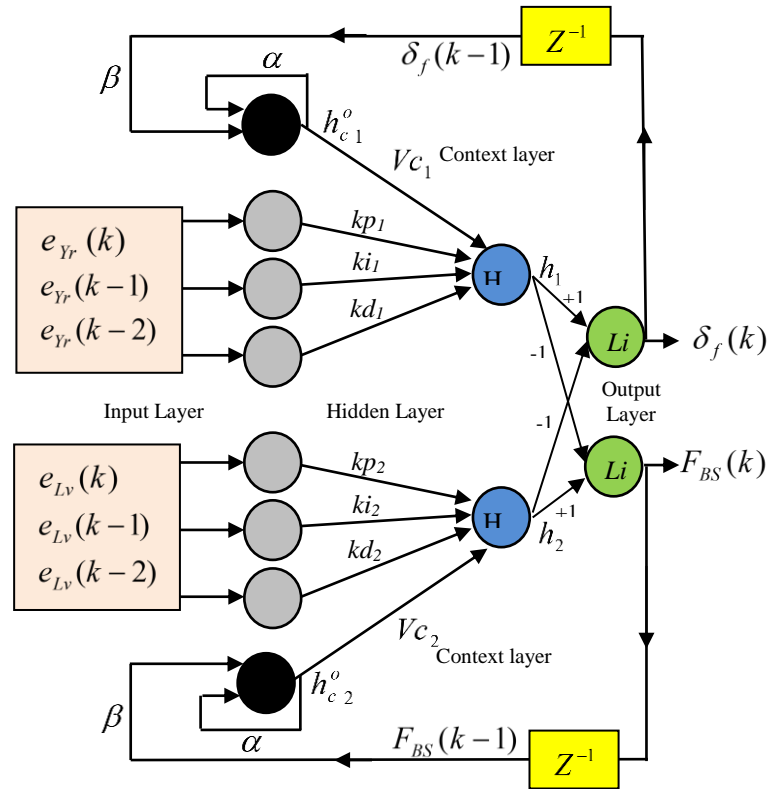
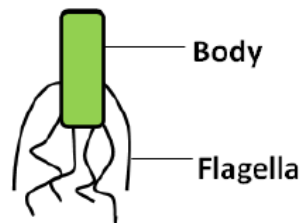


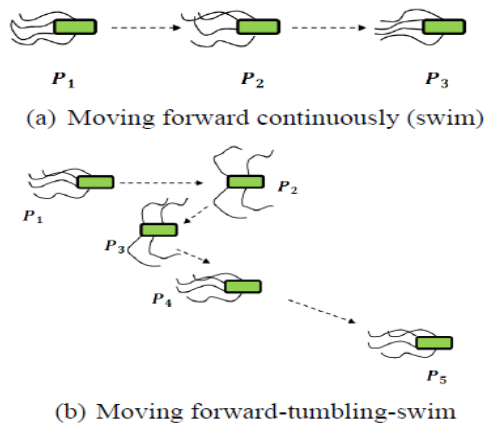
Figure 2. The structure of the proposed controller for 2DOF vehicle models.



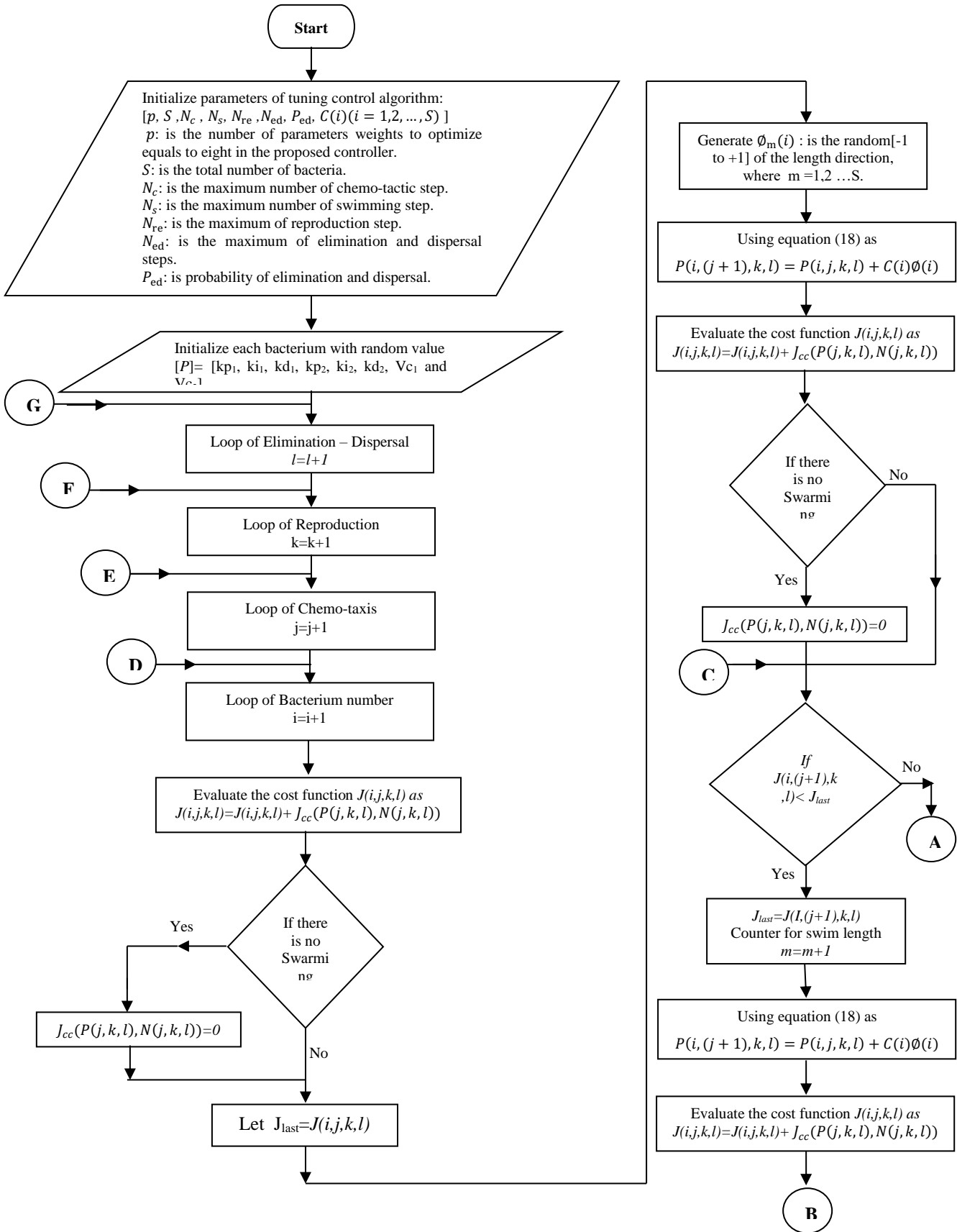
**Figure 3.** The proposed nonlinear MIMO-PID-MENN controller structure.



**Figure 4.** the structure of the bacterium.



**Figure 5.** kinds of E. Coli bacterium motion.



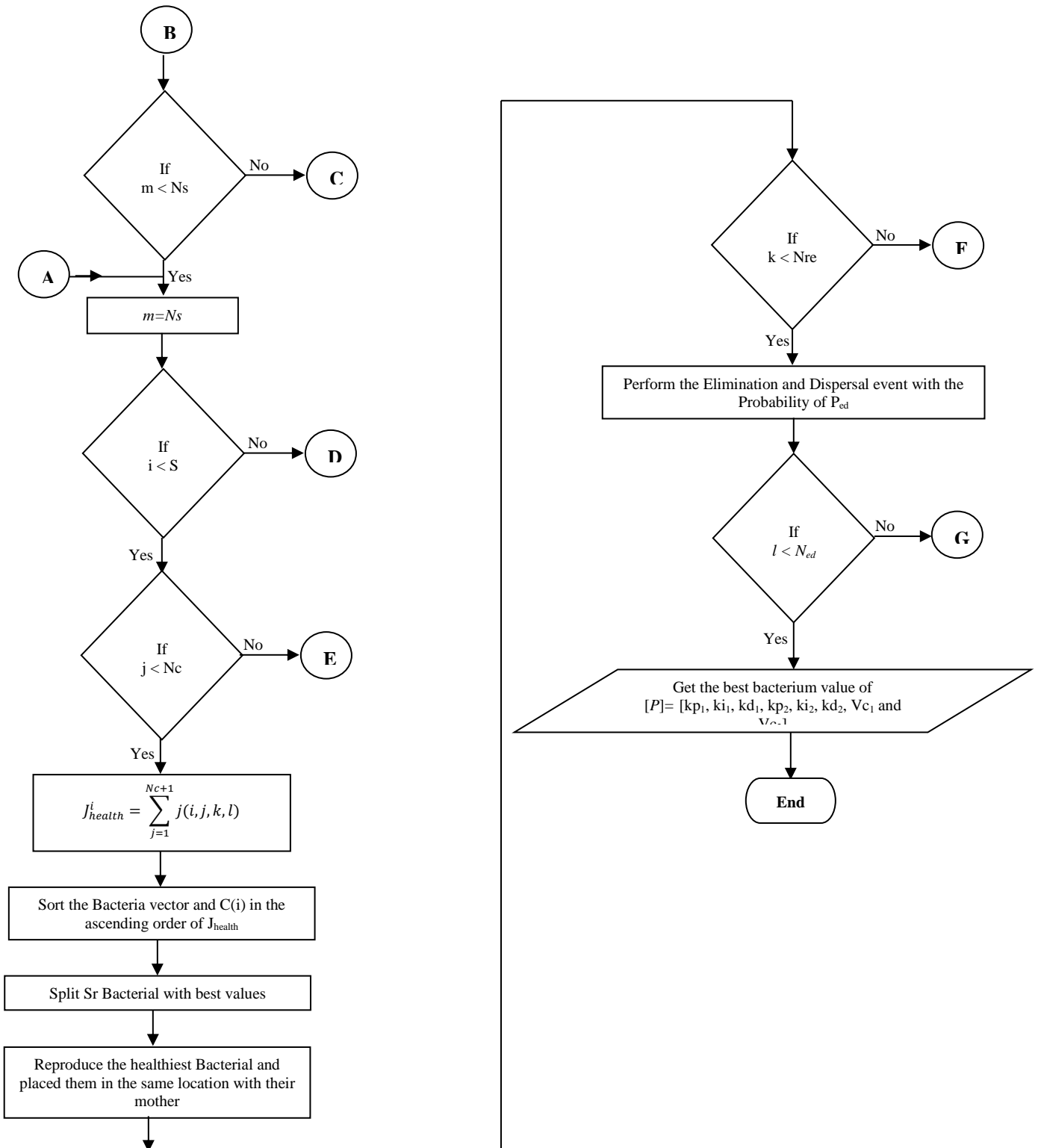


Figure 6. The flow chart of Bacterial foraging tuning control parameters algorithm.

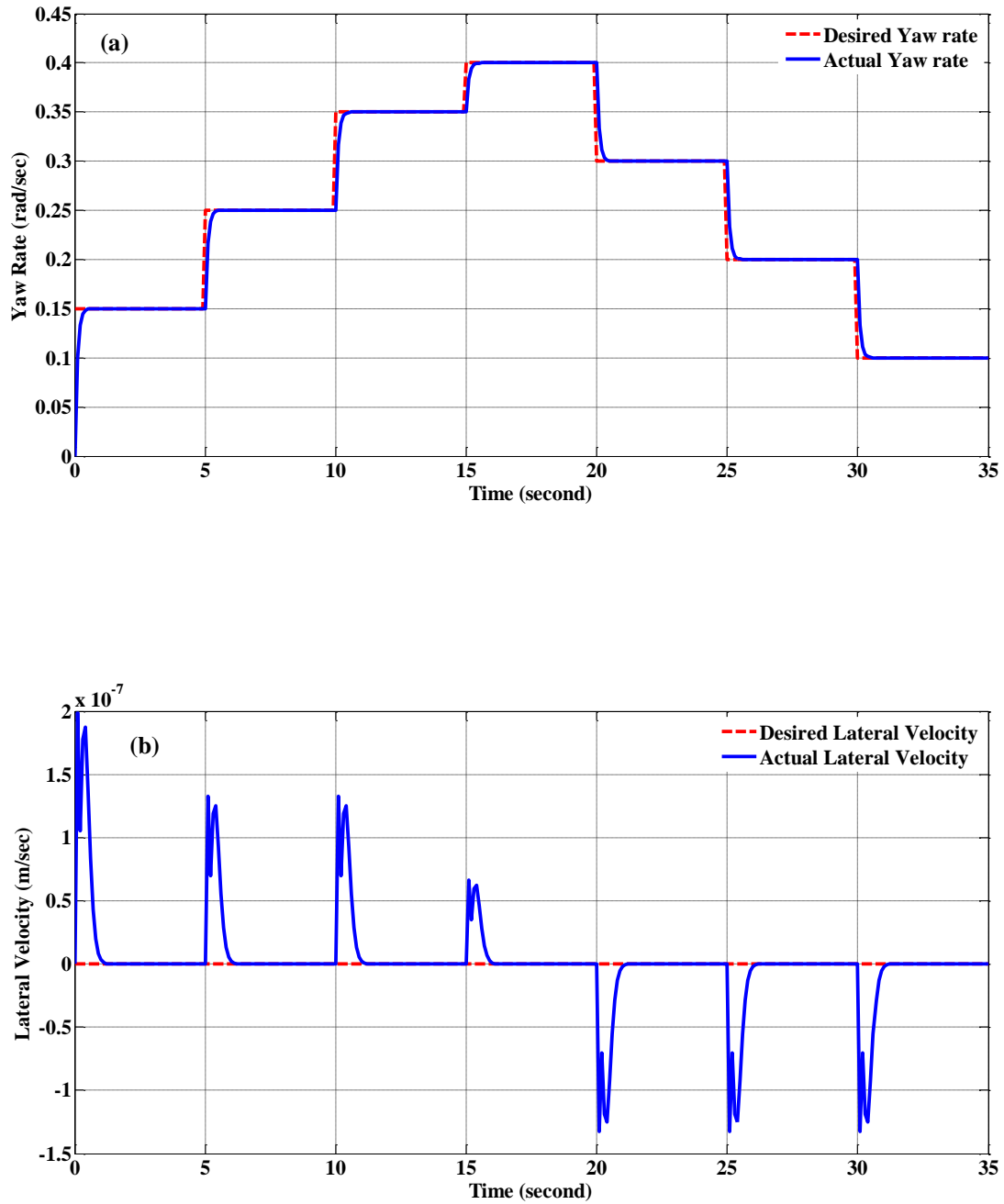
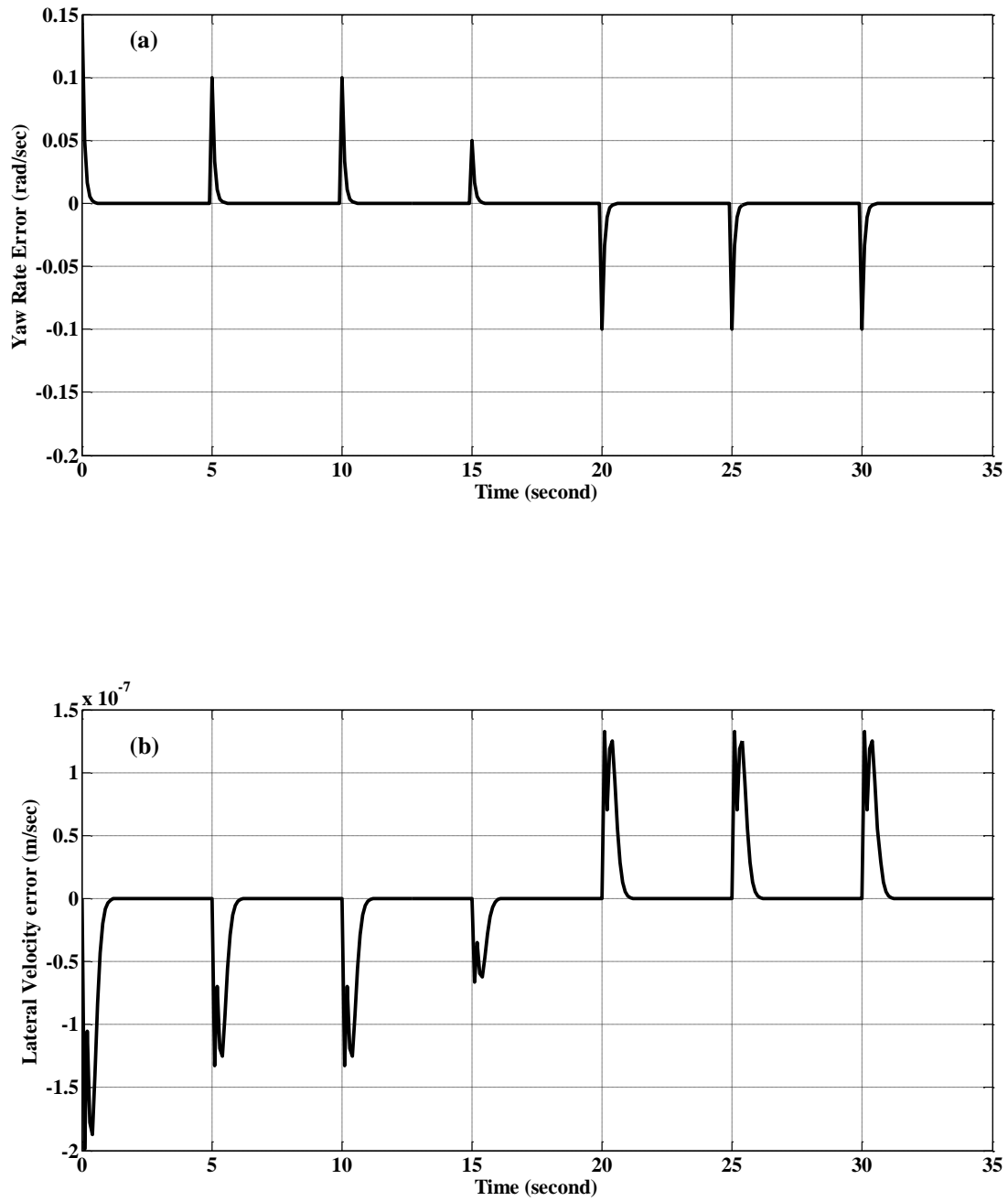
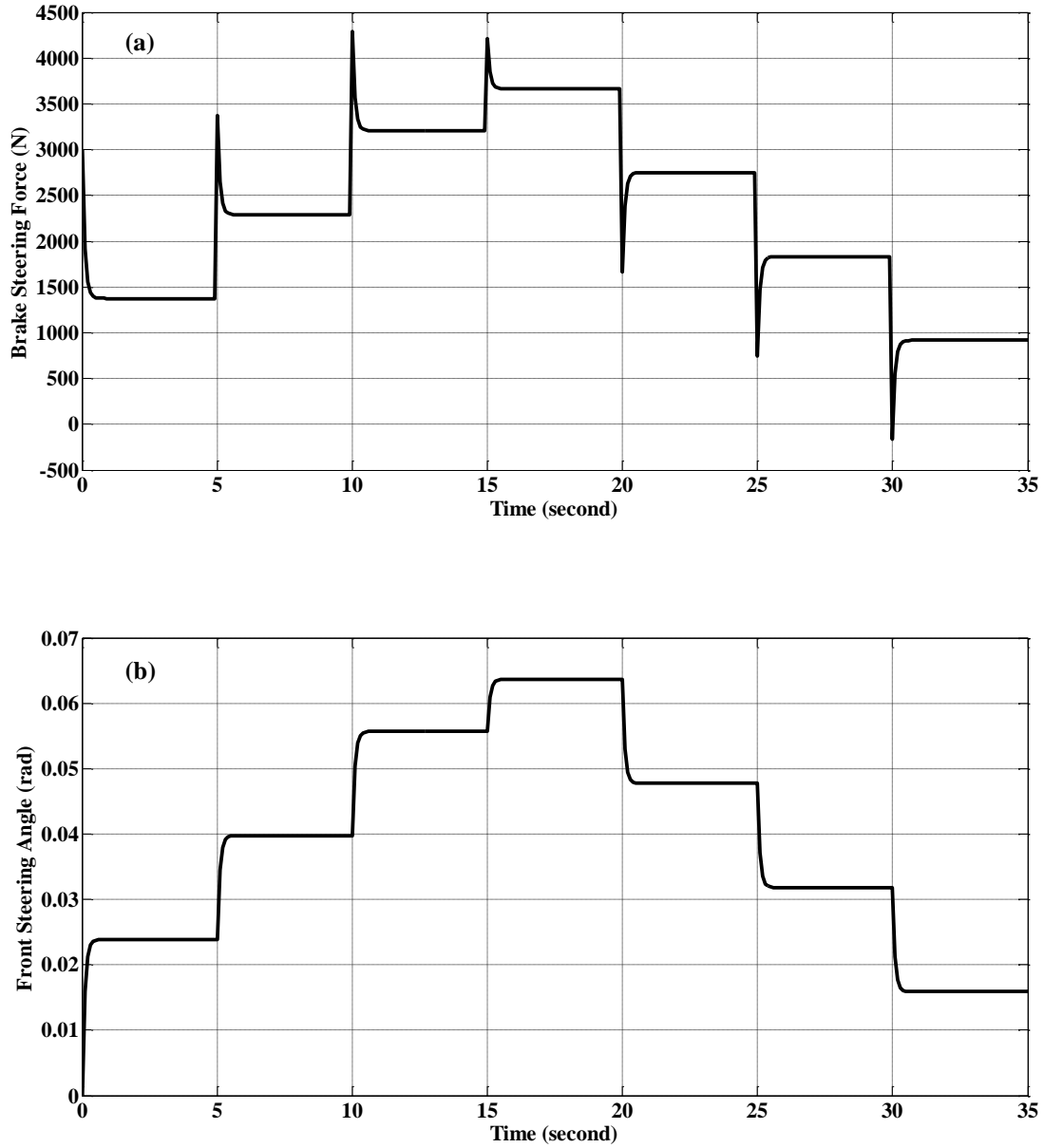


Figure 7. a) The response of the Yaw Rate (rad/sec); b) The response of the Lateral Velocity (m/sec)



**Figure 8.** The error signal between the desired and actual output of the vehicle model: a) yaw rate error signal; b) lateral velocity error signal



**Figure 9.** The actual output of the proposed controller a) the differential braking action; b) the front steering angle action.



**Table 1.** The parameters weights of the nonlinear MIMO-PID-MENN controller.

Vehicle Velocity	$kp_1$	$ki_1$	$kd_1$	$V_{c1}$	$kp_2$	$ki_2$	$kd_2$	$V_{c2}$
15	0.237	0.471	0.101	1.322	0.381	0.113	0.219	1.071
25	0.466	0.311	0.111	0.949	0.428	0.299	0.331	1.033
35	0.722	0.236	0.399	0.467	0.751	0.957	0.831	0.993
40	0.731	0.697	0.674	0.513	0.399	0.966	0.877	1.405
30	0.651	0.993	0.841	0.911	0.364	0.387	0.592	0.862
20	0.923	0.716	0.839	0.923	0.199	0.644	0.553	0.997
10	0.771	0.763	0.159	0.532	0.147	0.723	0.801	1.079

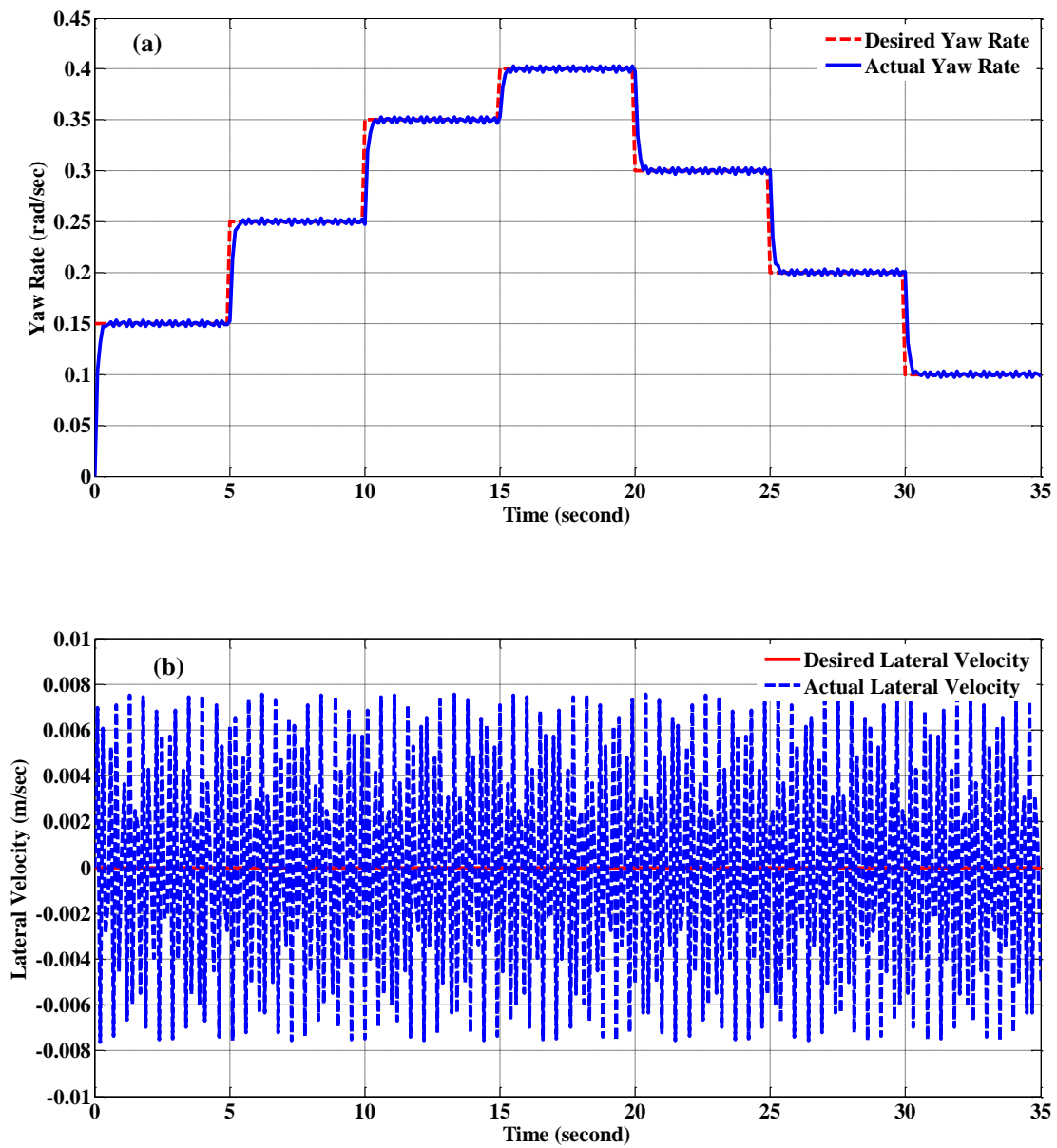


**Figure 10.** a) The response of the Yaw Rate (rad/sec) with disturbance effect; b) The response of the Lateral Velocity (m/sec) with disturbance effect.

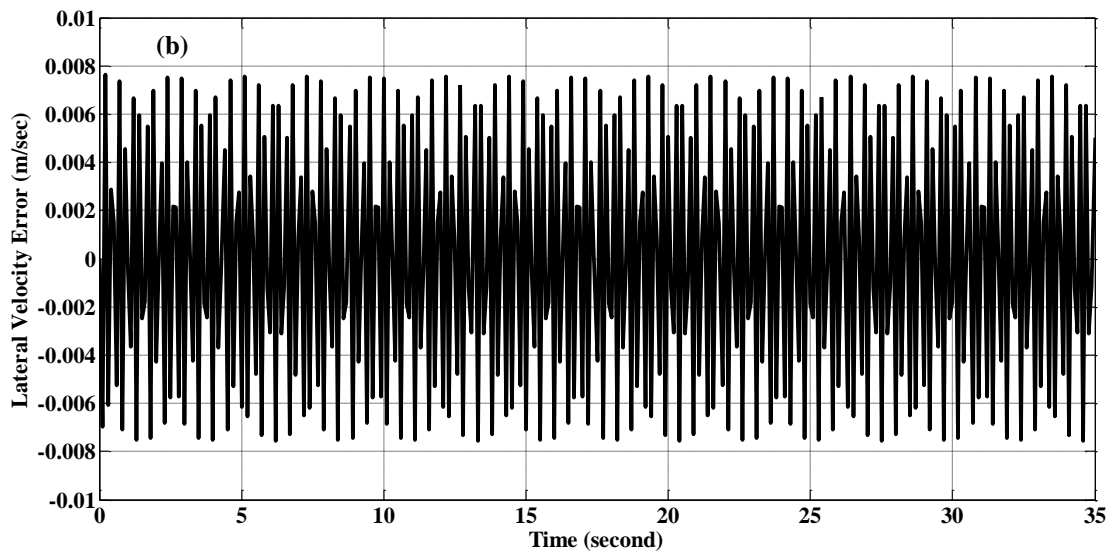
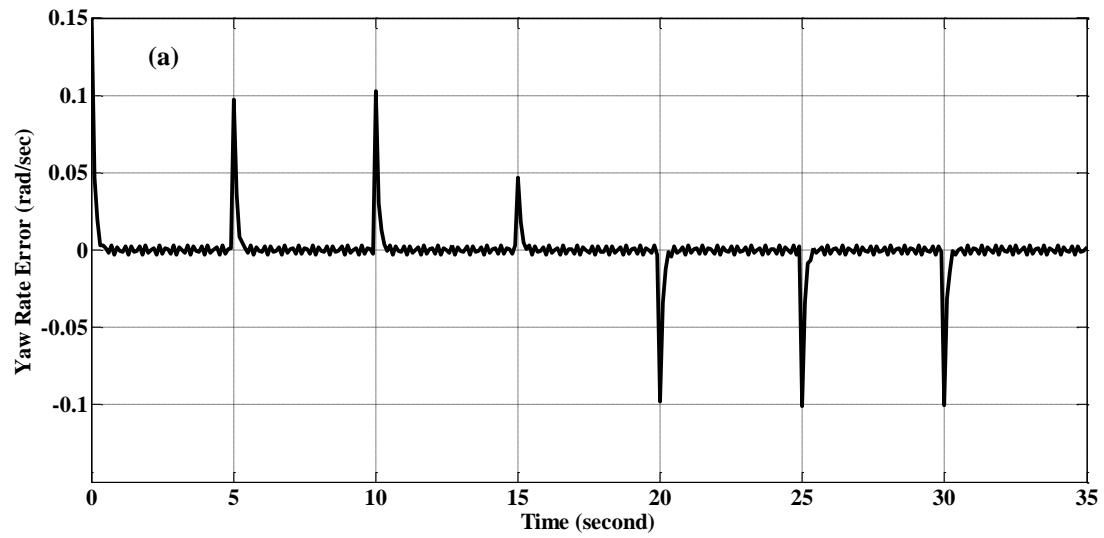


**Figure 11.** The error signal between the desired and actual output of the vehicle model with disturbance effects: a) yaw rate error signal; b) lateral velocity error signal

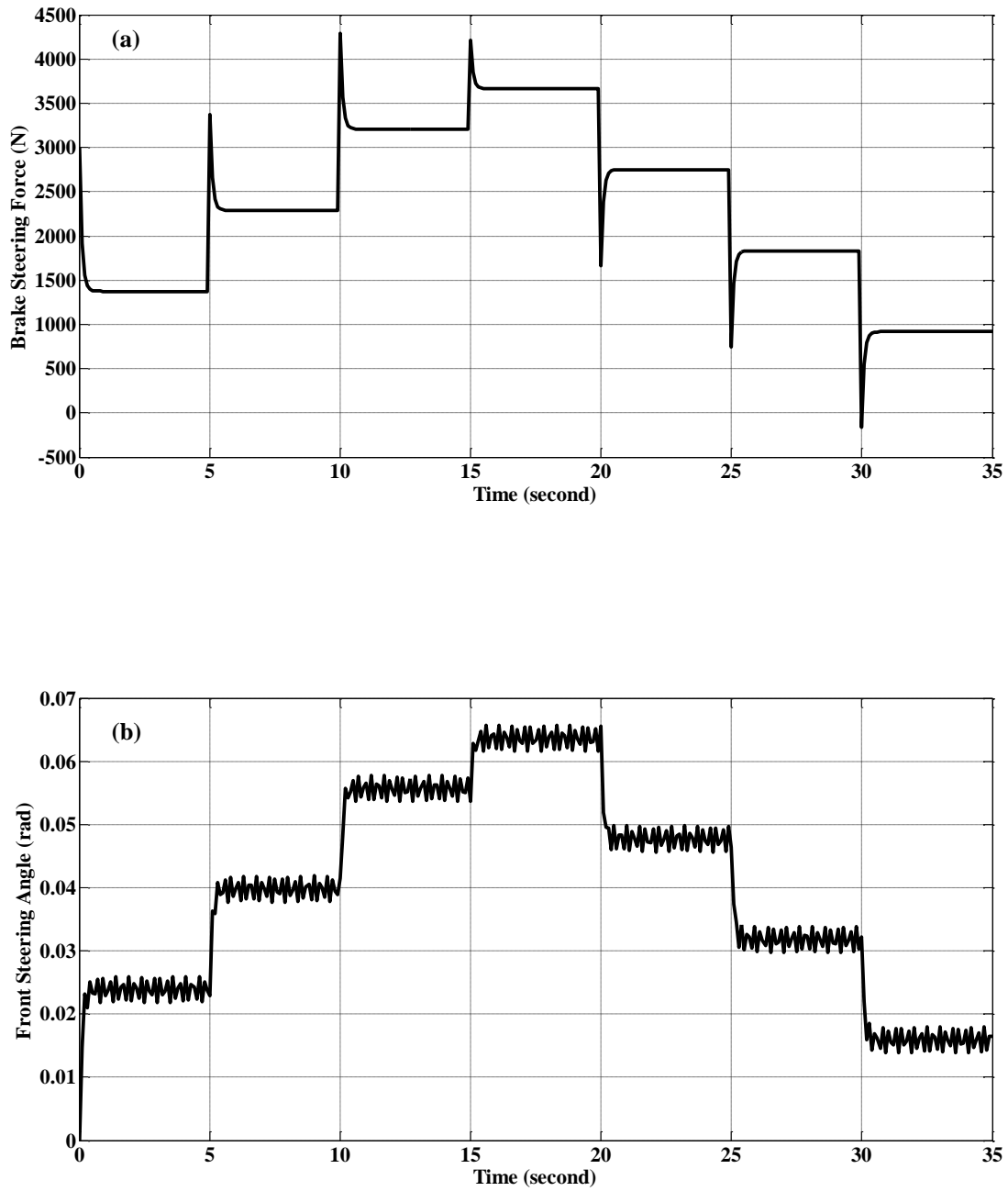


**Figure 12.** The actual output of the proposed controller with disturbance effects a) the differential braking action; b) the front steering angle action.